Universitat Politècnica de Catalunya
Escola Tècnica Superior d'Enginyeria de Camins, Canals i Ports

Departament de Matemàtica Aplicada III

Numerical simulation of failure involving multiple cracks with smoothed displacements

by

Marc Olm Serra

Master Thesis

Advisors: Elena Tamayo-Mas, Antonio Rodríguez-Ferran

Barcelona, May 2013

Abstract

Numerical simulation of failure involving multiple cracks with smoothed displacements

Marc Olm Serra

In this master thesis failure with smoothed displacements is studied. The goal is to understand how these models work with simple examples and reproduce an example with multiple cracks.

Firstly, the equations behind the general damage model are described. Here, the equations and the made assumptions are briefly presented. One simple example is developed to clarify all the process and have a good understanding regarding all the involved parameters. Then one example involving multiple cracks is developed. This example is intensively studied in order to illustrate the goodness of the proposed method with more than one crack, regarding applicability and limits.

RESUM

En aquesta tesina s'estudia el procès de fallida de materials amb desplaçaments regularitzats. L'objectiu és entendre com funcionen aquest tipus de models amb exemples simples i reproduir un exemple complex amb més d'una fissura.

Primerament, es descriuen les equacions darrera el model de dany. En aquest punt, les equacions i les hipòtesis del model són breument presentades. Un exemple és desenvolupat per clarificar i assolir un bon coneixement sobre el model contemplant tots els paràmetres involucrats. Després, un exemple amb més d'una fissura és desenvolupat. Aquest exemple és profundament estudiat amb l'objectiu de presentar la bondat del mètode emprat per a problemes amb més d'una fissura, contemplant l'aplicabilitat i els límits del mateix.

Acknowledgments

Primer de tot, m'agradaria expressar la meva gratitud cap a l'Elena Tamayo-Mas per haver-me ajudat setmana rere setmana durant tot aquest període de temps. Gràcies per la paciència, pels consells, per rebre'm amb un somriure cada dia. Gràcies també a Antonio per la predisposició a ajudar.

Gerard, Joana, Carlos, Carles, Arnau, Diana, i tots els que m'heu acompanyat durant aquests anys, vosaltres heu estat la universitat de veritat.

Gràcies a la meva família sencera pel vostre suport incondicional. Pare, mare, ells m'han ensenyat el valor de l'esforç. Gràcies per donar-me la oportunitat d' escollir el meu camí. Sense ells res d'això hagués estat possible. Josep Maria, per estar sempre allí.

I per últim m'agradaria fer-te una menció especial, per expressar tots els agraïments anteriors en una sola persona, gràcies Mercè.

Contents

List of Figures

List of Tables

Chapter 1

Introduction

This work deals with processes of damage and failure of materials [1], a basic knowledge in engineering since it may be found in most activities related to this field.

In this thesis a theory is presented regarding damage inception and growth. The process starts with a structure under load, in our case, a concrete one. The first stage, the elastic one, comes to an end when the most stressed point reaches the maximum stress that is able to hold. Afterwards, the material starts to behave in a different way, captured with the inception of the damage and its propagation as the damage increases while the load persists.

To numerically simulate this process, a continuum technique will be employed. If a local continuum technique is used, mesh dependence effect will appear [2], this is, the chosen mesh takes over control of the process, and the solution depends on the mesh. To solve this pathological mesh sensitivity and therefore to avoid unrealistic results, a regularization technique is used. There exist many regularization techniques, such as displacement interpolation [3] and nonlocal displacements [4],[5]. In this thesis, the regularization effect is incorporated into the model with an implicit gradient version [6] introducing nonlocal displacements. Higher order derivatives are added to the partial differential equation that describes the evolution of the nonlocal variable. The result is a smoothed displacements field that solves the pathological sensitivity of the mesh.

Even though what is previously presented may be a good technique for describing the failure process, this cannot be used in the final stage of failure [7]. Actually, when the damage is important through the structure the body is physically separated in two parts or more. This opening occurs at both sides of the most damaged points. It is time to change the strategy and leave the continuum technique, valid so far, and adopt a discontinuous technique that let us introduce discontinuities throughout the structure [8]. So, the resulting continuous-discontinuous technique leads to a more realistic description of the entire process.

In this thesis the first part of the process is described. Starting from the general theory for damage modeling [1], a continuous implicit gradient version [2] strategy is described. Damage inception and growth, regarding two examples of application (chapter 2) are deeply studied. The work ends with conclusions and recommendations for future work (chapter 3).

Chapter 2

Continuous model with smoothed displacements

2.1 Introduction. The need of a regularized media

A realistic numerical strategy should be able to represent the evolution of the damage through the process of failure of the material. This phenomenon is achieved by means of a constitutive law involving a particular damage law. The general form is known as a local model, where stress and deformations computed with a finite element technique in the node depend only on its own strain. Local damage models, based on [2] :

- Allow a differential format of the constitutive equations.
- Are valid for damage problems where the displacements field and stresses vary smoothly throughout the body.
- Are violated if the damage process takes place in a vanishing volume.

The first condition is basic for FEM formulation and is accomplished, but the second one is barely accomplished in our case of study. There is found to be a large stress difference between different areas giving a solution far from a smoothed one, so the nodes that are selected to compute the results are very important. In fact, with a continuum model the numerical simulations strongly depend on these nodes, and therefore they present a pathological mesh sensitivity. Hence physically unrealistic results may be obtained since they will completely depend on the chosen mesh.

The third one is never accomplished with local models, and together with the second one drives to the main issue, the pathological mesh sensitivity. The strain localization is found in the smallest element entering softening regime. It means that the material affected by damage is localized in a row of elements, so the solution completely depends on the element size and therefore on the mesh. Thus, when the element size tends to zero, so does the localization band size and it results in a vanishing volume affected by damage. If a vanishing volume is affected by damage, a finer mesh gives a decreasing dissipation of energy as

the damage occurs in a vanishing volume. This is a big problem, because in the extreme case, an infinitesimal element size, the dissipated energy would be zero [9]. The goal is to avoid this mesh dependence and make the solution be independent from the chosen mesh regarding the same problem.

To solve this problem, a regularization technique may be used. The idea of the regularization technique is to introduce other nonlocal displacements [4], involving neighborhood effects for the computation of each point strains. The goal is to achieve a smoothed field of displacements in order to avoid mesh sensitivity and make the technique be independent from the mesh.

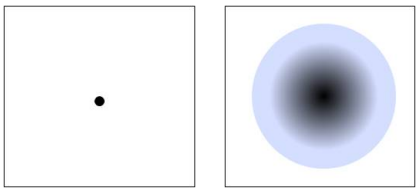

(a) local action (b) nonlocal action

Figure 2.1: Nonlocal action idea

Nonlocal models are used to avoid mesh pathologies. Otherwise the analysis may not be physically correct. Including nonlocality effects we achieve [2] :

- Smooth deformations.
- Avoid localization problems in a surface and therefore mesh dependence.

There are many techniques that allow us to include nonlocal effects in our problem. In our case of study this effect is achieved by means of the gradient version of the nonlocal model, see the extended method in [6].

2.2 Model

In this section the gradient version of a nonlocal damage model used to develop the incoming work is presented. Many authors deal with this technique [2],[4],[7], and here just a summary of the equations is presented.

2.2.1 Overview of the implicit gradient version

In the following, the most significative equations and laws for the model are described.

Constitutive law

The governing equation for mechanics deformation

$$\nabla\sigma(\mathbf{x},t) = 0 \tag{2.1}$$

is considered where σ is the stress tensor. Then, the general expression for the constitutive law in solid mechanics is introduced as

$$\sigma(\mathbf{x},t) = \mathbf{C} : \varepsilon(\mathbf{x},t) \tag{2.2}$$

where ε is the strain tensor. The stiffness tensor $\mathbf{C}$ that gives the relation between stresses and strains is affected by a damage index in

$$\sigma(\mathbf{x},t) = (1 - D(\mathbf{x},t))\mathbf{C} : \varepsilon(\mathbf{x},t) \tag{2.3}$$

where $D(\mathbf{x},t)$ is the damage index that affects the global response of the material. This index is set to 0 if no damage is observed, and monotonically grows up to 1 with the stress and deformation growth. Described in this thesis with an exponential law, it never reaches the value of 1. Therefore,

$$D \in [0,1) \tag{2.4}$$
$$\dot{D} \geq 0. \tag{2.5}$$

A high damage index makes the global stiffness of the material decrease, giving large deformations with any load value. Local strains are computed as the symmetric gradient of the displacements field

$$\varepsilon(\mathbf{x},t) = \nabla^s\mathbf{u}(\mathbf{x},t). \tag{2.6}$$

Here is where the nonlocal property is first introduced. This model calculates the nonlocal displacements $\tilde{\mathbf{u}}$ involving the local displacements $\mathbf{u}$ in the second-order partial differential equation

$$\tilde{\mathbf{u}}(\mathbf{x},t) - {l_c}^2\nabla^2\tilde{\mathbf{u}}(\mathbf{x},t) = \mathbf{u}(\mathbf{x},t) \tag{2.7}$$

where l_c is the characteristic length of the nonlocal damage problem, parameter introduced that controls the regularization effect. This equation gives the name to the method, since the gradient operator affects the natural displacements in the described way . The implicit version of the method is regarded, existing the explicit one [2]. Then, nonlocal strains equation involves nonlocal displacements

$$\varepsilon_{NL}(\mathbf{x},t) = \nabla^s\tilde{\mathbf{u}}(\mathbf{x},t). \tag{2.8}$$

Now the nonlocal state variable is defined in terms of nonlocal strains

$$\mathbf{Y_{NL}}(\mathbf{x},t) = \mathbf{Y}(\varepsilon_{NL}(\mathbf{x},t)) \tag{2.9}$$

so the damage evolution is also affected by the nonlocal state variable

$$D(\mathbf{x},t) = D(Y_{NL}(\mathbf{x},t)) \tag{2.10}$$

Governing equation (2.1) for solid mechanics together with Eq.(2.7) and its discretization from the weak form leads to a finite element formulation problem [6] where solutions for $\mathbf{u}$ and $\tilde{\mathbf{u}}$ may be obtained.

Damage exponential law

It is assumed that our parameter D for damage depends on the state variable Y

$$D(\mathbf{x},t) = D(Y(\mathbf{x},t)) \tag{2.11}$$

where state variable Y is defined here by means of the truncated Rankine criterion

$$Y(\mathbf{x},t) = \sum_{i=1}^{3} \max\{0,\sigma_i\}, \tag{2.12}$$

where $\sigma_i, i = 1,2,3$, are the principal effective stresses. Then the softening branch is controlled by the imposed softening exponential law. This law is based on [3]. It is initialized when the state variable reaches the value of the tensile strength. Thus, it starts when $Y_0 = \sigma_0$. It is written

$$q(Y) = Y_0 e^{(-2H_S\left(\frac{Y-Y_0}{Y_0}\right))}, \quad Y \geq Y_0 \tag{2.13}$$

where $H_S \geq 0$ is the softening parameter. H_S is given by

$$H_S = \frac{b}{\mathcal{L}-b}, \quad \mathcal{L} = 2\frac{EG}{{\sigma_0}^2} \tag{2.14}$$

where b is the width of the localization band, the assumed width of damaged elements for a crack path and $\mathcal{L}$ is the mechanical length of the material. E, G, σ_0 are the Young modulus, the fracture energy and tensile strength respectively. From the definition of the exponential law and its softening parameter, theory says that it cannot be negative, hence

$$H_S \geq 0 \quad \Rightarrow \quad b < \mathcal{L}. \tag{2.15}$$

Note that the softening parameter is introduced depending on properties given by the material and the mesh, therefore on the particular simulation.
From Eq.(2.13) the damage index is defined in terms of the corresponding current value of damage, once above the damage threshold

$$D(Y) = 1 - \frac{q(Y)}{Y} \quad Y \geq Y_0. \tag{2.16}$$

Therefore damage starts from the damage threshold Y_0 and monotonically increases such that never reaches value of 1. In figure 2.2(b) σ/ε resulting law is shown.

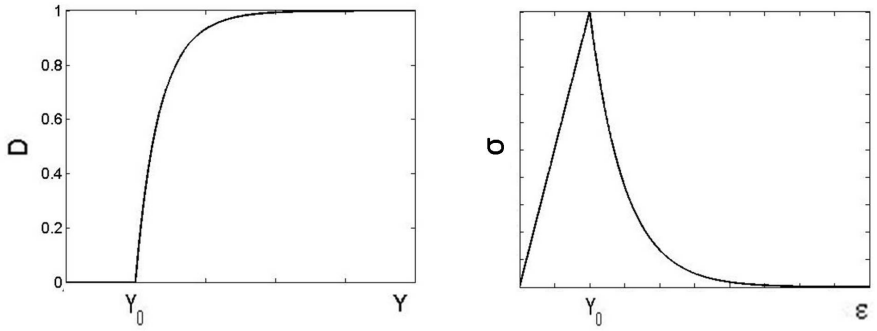

(a) Damage-state (b) Strength-strain

Figure 2.2: Exponential law

Boundary conditions

In this problem mechanical boundary conditions for the governing equation must be given. Also boundary conditions for the regularisation equation 2.7 must be defined. Mechanical boundary conditions are described for each case, but regularisation boundary conditions are discussed here. These ones, regarding [7], could be Dirichlet boundary conditions [4], prescribing the nonlocal displacement equal to the local displacement in all the domain boundary, this is

$$\tilde{\mathbf{u}} = \mathbf{u} \quad \text{on} \quad \partial\Omega. \tag{2.17}$$

But with Eq.(2.17) there is no regularization on $\partial\Omega$. Discussed in [10], this may be solved prescribing Neumann boundary conditions for Eq.(2.7).

In this gradient nonlocal damage model, non-homogenous combined boundary conditions are used in order to regard the regularization problem on the boundary of the domain. As seen, the motivation for that is the difficulty of achieving satisfactory results just with Dirichlet or Neumann boundary conditions. Particular combined boundary conditions are written as

$$\begin{cases} \tilde{\mathbf{u}} \cdot \mathbf{n} & = & \mathbf{u} \cdot \mathbf{n} & \text{on } \partial\Omega \\ \nabla(\tilde{\mathbf{u}} \cdot \mathbf{t}) \cdot \mathbf{n} & = & \nabla(\mathbf{u} \cdot \mathbf{t}) \cdot \mathbf{n} & \text{on } \partial\Omega \end{cases} \tag{2.18}$$

where $\mathbf{n}$ is the directional normal to the boundary $\partial\Omega$ and $\mathbf{t}$ is the direction tangent to the boundary $\partial\Omega$. So we will specify in one hand mechanical boundary conditions and in the other hand the regularization boundary conditions. With these boundary conditions, the same normal displacements are imposed.

2.3 Simple crack analysis: validation of the codes

2.3.1 Three point bending test analysis (3PBT)

In previous sections the main model has been presented and treatment of equations has been developed. Here starts the computational work, and the first proposed stage is a validation of the model with a simple test. For this purpose, a simple three point bending test, hereafter 3PBT, has been chosen. This example is selected because it represents a well studied and known behavior [11]. This example regards simple boundary conditions and applied loads, and presents an isostatic deformation, that should not be hard to capture.

This example is a plane-strain notched beam subjected to a concentrated load in the middle of the top edge. Geometry is depicted in figure 2.3. Due to similarity with the main test of this thesis, dimensions have been chosen near the dimensions of that one. Dimensions of the beam are $L = 100$ cm x $H = 30$ cm. The length and width of the notch are b= 10 cm and a= 2 cm respectively. For this first example, thickness of the beam is set to the unit, so the obtained forces are forces per unit. The load is applied at the central point of the top edge by imposing vertical displacements in compressive direction. The left bottom point acts as a fixed boundary, with both vertical and horizontal displacements restricted while the right bottom point acts as a roller boundary condition, where just vertical displacement is set to 0.

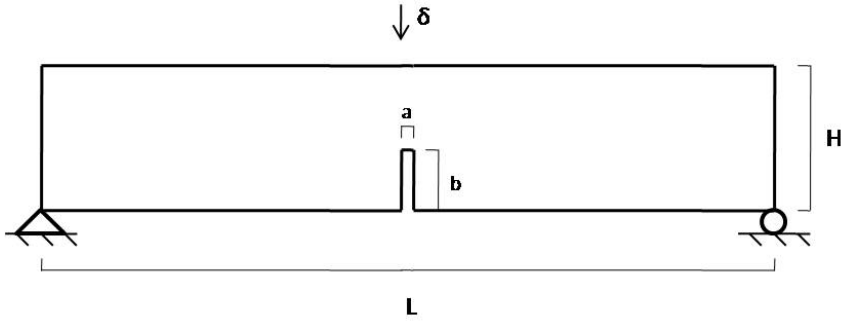

Figure 2.3: Geometry for 3PBT

The problem is solved aided by an arc-length strategy. In this arc-length strategy a variable displacement is imposed in the point where the punctual force is applied. This displacement increases or decreases depending on convergence requirement. In table 2.1 material properties are described.

As seen before the problem is mainly controlled by two parameters added in the formulation, the damage law by means of the band size width b and the characteristic length l_s. Band size has a theoretical limit, described in Eq. (2.15). For this simple example a value of b=0.2 is selected.

Property	Notation used	Value
Young Modulus	E	30 GPa
Poisson ratio	ν	0.2
Tensile strength	σ_0	2 MPa
Fracture energy	G	100 J/m^2

Table 2.1: Material properties for the 3PBT

The computational domain is discretized with quadrilateral elements with the mesh generator **ez4u**. The analysis is carried out with an average mesh size in the central part of 10 mm, since here the purpose is just to evaluate and validate the current codes, not regarding mesh dependence. The right bottom support is simply supported and therefore horizontal displacement is allowed along this direction. Vertical displacement is imposed to be null here, like in the left bottom support, that corresponds to a typical embedment boundary condition. In figure 2.4 typical deformation for this process is shown. The background mesh is plotted in yellow and shows the original mesh, while the black one shows the deformed mesh. This deformation corresponds to the damage depicted in figure 2.6(b), where displacements are drawn amplified by a factor of 100 times.

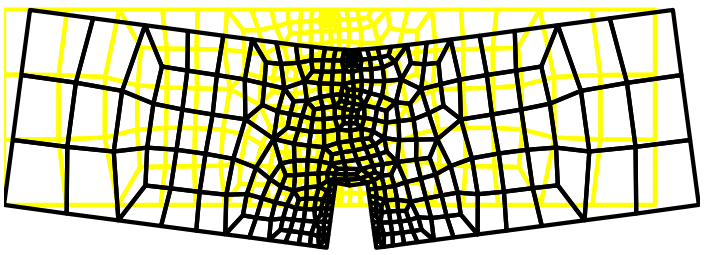

Figure 2.4: Deformation for 3PBT

An analysis with different l_s is carried out in order to appreciate the effect of the characteristic length of the problem. First of all, it is important to appreciate the difference

between a model with l_s=0, equivalent to a local model since there is no smoothing in displacements, and another model computed with a value for l_s different from 0.

From this moment and onwards, the color scale depicted in figure 2.5 is used for the damage index in plots. The plotted area for this problem is not the full length of the beam, since the damage occurs just above the notch. Thus, the damage plots show the central part of the beam. A length of 22.5 cm is depicted from the central symmetric axis of the beam towards right and left edges. Therefore damage figures dimensions are full width and a length corresponding to a central part of 2 x 22.5 = 45 cm.

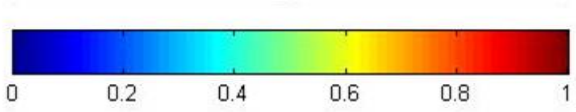

Figure 2.5: Colorbar used in all damage plots

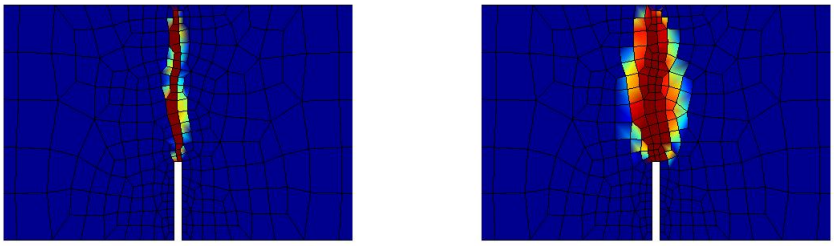

(a) local solution (b) smoothed solution (l_s=0.2)

Figure 2.6: 3PBT: local-smoothed

Damaged elements for the first simulation are clearly found in a row of elements. Typically this is the damage observed for local models and its main problem. The damage is located within a column of elements growing in the direction affected by most stress.

As shown in figure 2.6, the computed crack follows a straight path starting from the tip of the notch and grows upwards with the increasing imposed displacement. It goes on towards the load application point to complete a straight band of damaged material that remains vertical. The process is isostatic and involves just rotation around the load application point affecting mainly the elements located in the line connecting the top and the tip of the notch, which are clearly in traction in the horizontal direction. As the damage grows, the damaged area presents a loss of stiffness up to be almost zero and lets the non-damaged area above

take the efforts. The end of this process comes with the central band completely damaged ($D \backsimeq 1$).

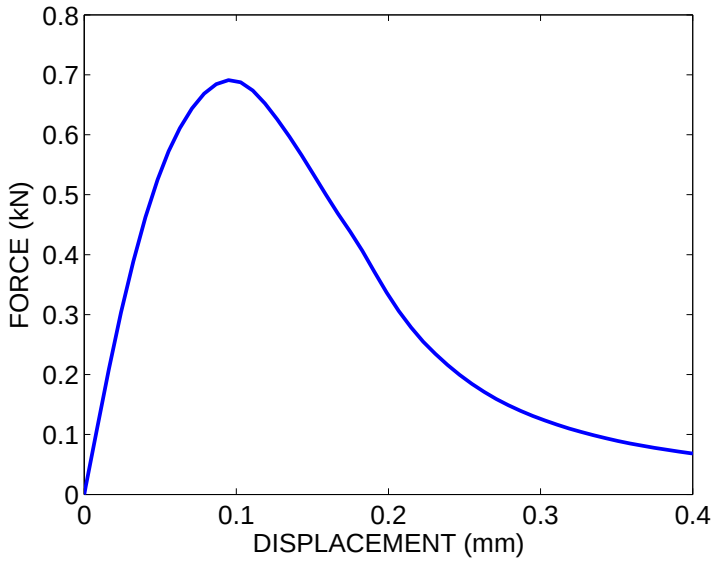

Figure 2.7: 3PBT: Force-deformation

Plot 2.7 shows the force-deflection curve for figure 2.6(b). In this plot, the elastic range of the material may be seen. This is the deformation up to reach the threshold where the damage strategy is activated by means of the truncated Rankine model involving the three principal strains, Eq. (2.12). This ratio is related to the elastic modulus (Young modulus) of the material. From this point, the damage provokes the softening branch of the curve. It results in a decreasing strength while the deformation increases.

It is observed that with local models, with l_s=0, the damage band is found in a row of the smallest size elements. Adding nonlocal displacements, this is $l_s \neq$0, damage occurs in more than one element, depending on the characteristic length value. This regularisation effect is controlled by the Eq. (2.7).

2.3.2 l_s and b parameter with 3PBT

Nonlocal processes depend on two parameters that have been added during the formulation, b and l_s. First of all, it is important to clarify that our objective is to model by means of l_s, with a fixed damage law affected by b. Therefore our efforts are focused on how l_s affects the model, but here the damage band size behavior is also studied in order to understand its contribution.

Detailed in section 2.2.1, b affects the order of the exponential law, introduced in Eq.(2.14) and l_s is added with the nonlocal displacements, in Eq.(2.7).

Characteristic length (l_s) in 3PBT

The effect of the nonlocal displacements is increased by the use of l_s parameter. Coming from low values, that give solutions close to local models and up to high values that give a scattered damage plot resulting from a excessive spreading of the damage. In terms of the model, an excessive regularisation effect that makes the solution be completely smoothed but physically unrealistic. The visual experience, the knowledge of the model and the comparison between real experiments and numerical simulations will tell us where the limit for obtaining realistic results is, and those range of values that suit the most a realistic solution.

In figure 2.8, different analysis are carried out with increasing values for l_s.

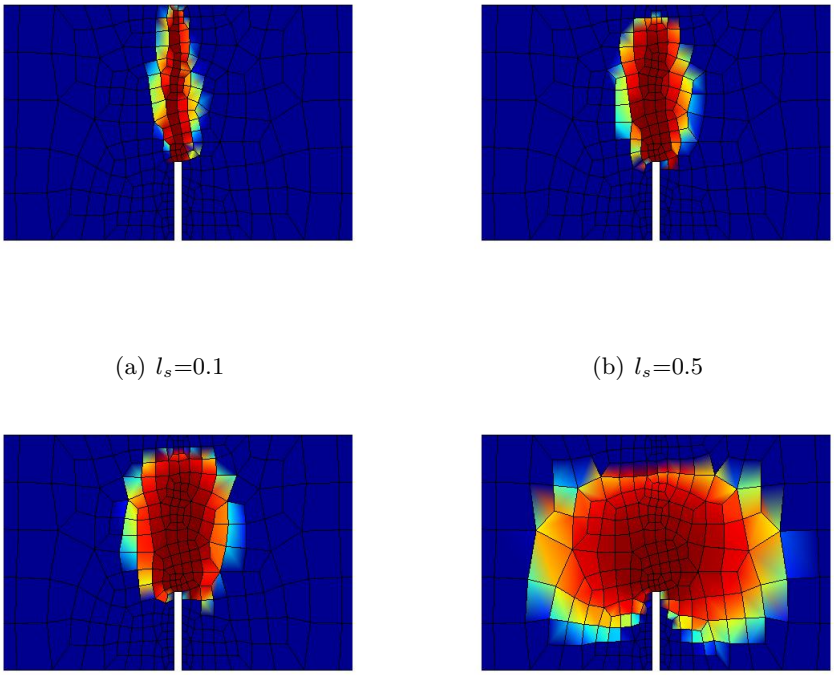

(a) l_s=0.1 (b) l_s=0.5

(c) l_s=1 (d) l_s=5

Figure 2.8: Damage plots depending on l_s for 3PBT

Each value for l_s gives a different curve for force-deformation ratios, the curve that explains all the stress-strain process through the deformation process.

The regularization effect of the nonlocal displacements tries to overlay the solutions for the same problem but with a different mesh (mesh dependence). In this case it is checked whether the characteristic length is important or not and which values fit the problem most. Higher characteristic lengths give higher dissipated energy, this is planer softening branches.

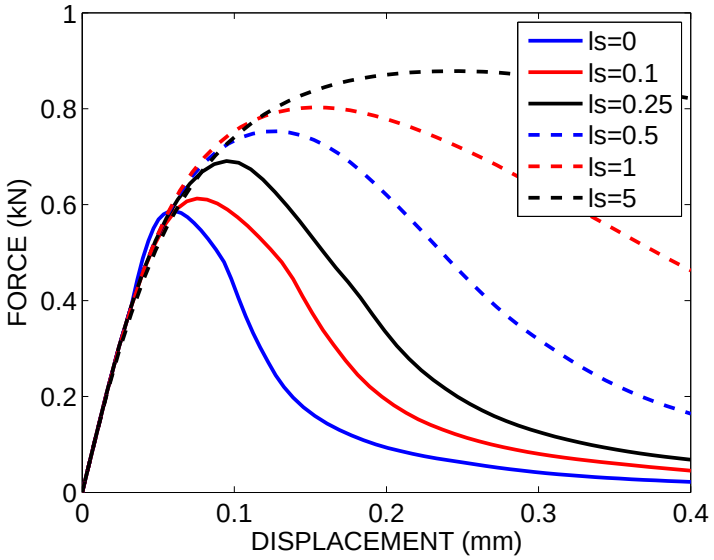

Figure 2.9: Different l_s

This happens due to the regularization effect of the model. With a major contribution of the nonlocal displacements, the number of elements affected by the damage will increase in the nearby of the original ones due to this spreading character. The higher the value is, the most regular damage plots are observed.

For this example and from the explained above, visual inspection says that the range of values for the characteristic length that suit the most our problem are those ones around $l_s = 0.2$.

Damage band width (b) in 3PBT

Width of the damage band is defined to get the damage law. This parameter is generally given by two times the average size of the elements involved in damage. In our case, the mesh is created with an average mesh size of 10 mm in the central area, therefore the theoretical value would be $b = 20$ mm. As seen, it is a parameter based on the element size of a particular mesh and should be adapted to every mesh. In this work it will be treated as a fixed value since the objective is to appreciate the characteristic length influence and its goodness in avoiding for itself the mesh dependence.

However, different analysis involving different values for b are developed here to clarify its influence on the problem. The goal is to observe whether the selection of this parameter may affect the calculations. Geometry and material properties are the same ones as before, detailed in section 2.3.1.

The damage plots show a clear dependence on the selected value for the damage band size. Reminding Eq. 2.13 the band size affects the exponent of the damage law. Resulting

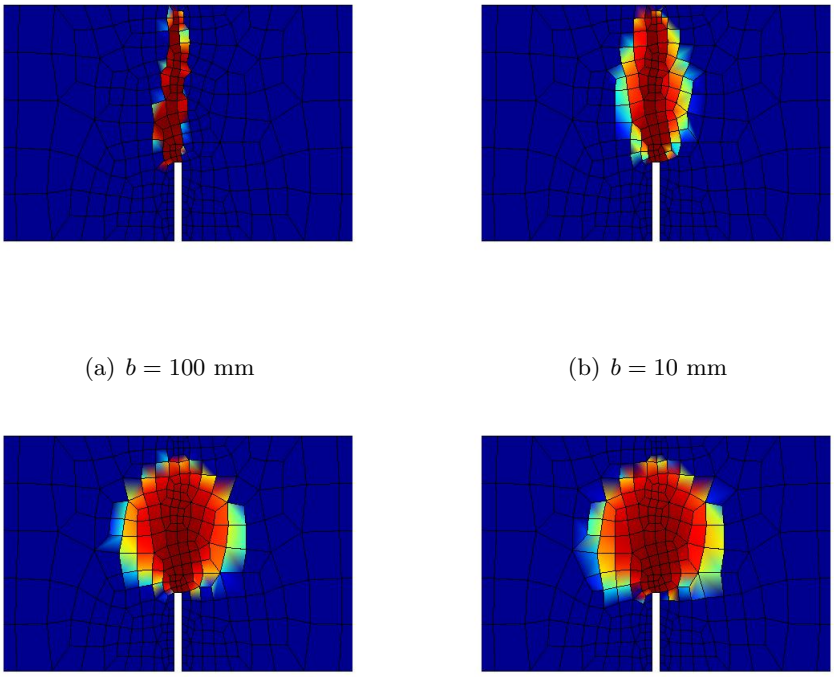

(a) $b = 100$ mm (b) $b = 10$ mm

(c) $b = 1$ mm (d) $b = 0.1$ mm

Figure 2.10: Damage plots depending on b for 3PBT

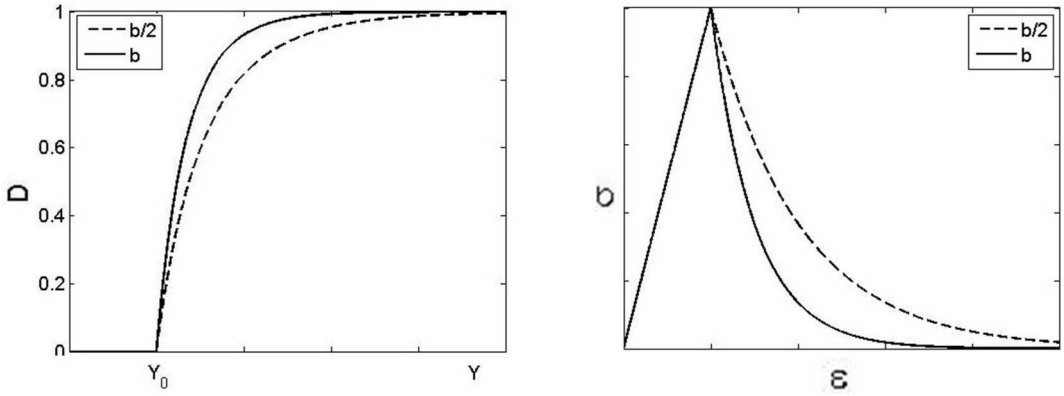

(a) Damage-state (b) Strength-strain

Figure 2.11: Influence of b in damage laws

damage law for different values of b is shown in figure 2.11.

From the damage plots and the theory explained above, band size affects the damage making it higher with low values of the parameter. The explanation for this is that with a softer damage law, the main stiffness of the material is kept because the damage increases slowly. This situation spreads the damage and makes the elements next to the damaged ones take damage. On the other hand, with high parameters the damage acts fast and in early stages for the deformation, so the damage is located in a small surface. The force-deflection plot for this situation is depicted in 2.12.

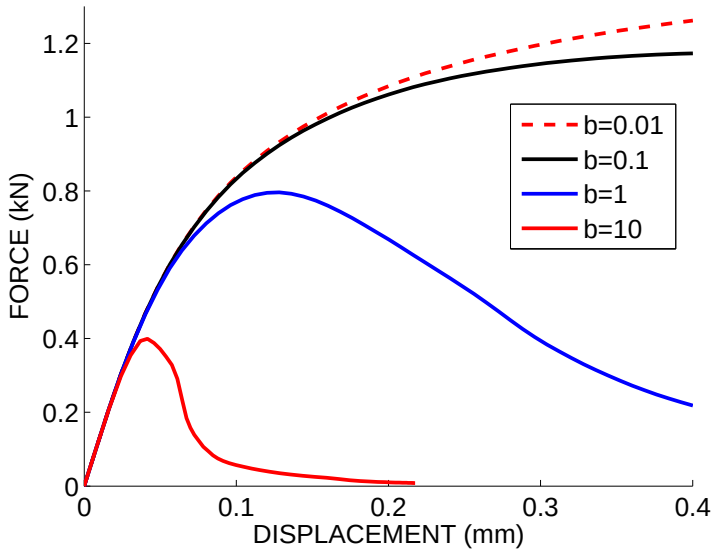

Figure 2.12: Different b

In summary,

- l_s acts like a scatterer and involves nodes in the nearby to compute a smoothed displacement for each node so the final result is smoother than a local model. The higher the value of the parameter is, the smoother result is obtained. This effect is globally observed with a soften of the softening branch of the force-displacement curve.

- b acts modifying the damage evolution in the problem. With higher values the damage grows faster, and therefore the deformation and loss of stiffness process is found in earlier deformations, with few elements damaged. When the value is given lower values the damage grows slowly but carrying a high load, hence damage is more scattered and the curve of the softening branch results softer, always with higher deformation.

2.4 Multiple crack analysis

So far the resolution technique has been developed for a simple example, the 3PBT. Now we turn on a multiple cracks analysis involving a geometry where more than one crack is tried to be captured, the main goal of this thesis.

2.4.1 Presentation of the problem

This example is based on [3]. The presented case consists of a plane-strain doubly notched beam subjected to four point bending (4PBT). In figure 2.13 the geometry of the problem is depicted. Dimensions of the beam are a width of 134.0 cm and a height of 30.6 cm. An amplitude of 30.6 cm is chosen to make the section be squared. Two notches of $b = 8.2$ cm x $a = 0.5$ cm are considered in the middle of the beam. The load is applied in the central supports, considered to be rigid and disposed symmetrically at 8.0 cm from the center of the beam. Vertical displacements of opposite sign are imposed at the top and bottom supports in order to compress the beam and produce bending. These supports are rigid since their function is just to transmit the applied load to the beam and avoid damage problems related to load applied in a unique point. The two supports near the extremes of the beam (located at 20.3 cm from these ones) are fixed. All supports along the beam have the same dimensions, they are squared supports of 4.0 cm x 4.0 cm.

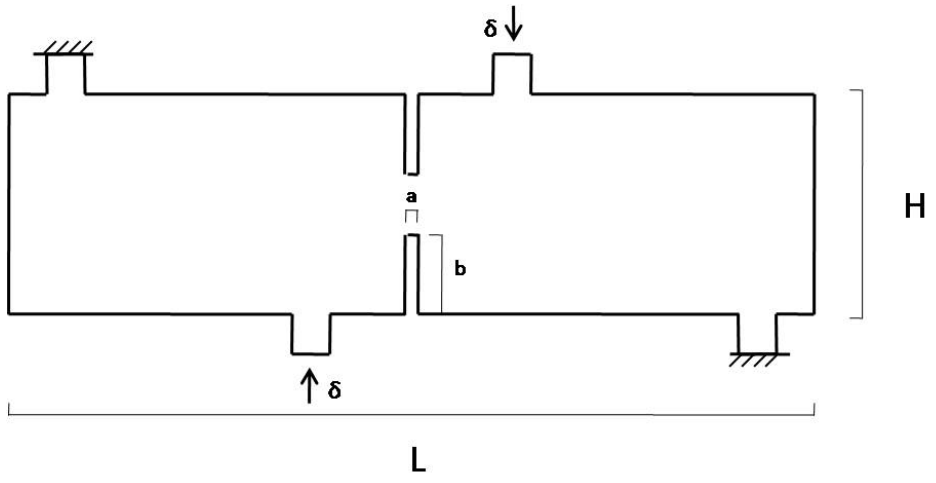

Figure 2.13: Geometry for 4PBT

Material properties and are detailed in table 2.2.

The problem that is going to be studied regards a four point shear stress problem, this is a beam subjected in two points and load applied in two more points in order to produce shear stress in controlled areas along the beam. This case is selected due to its symmetric conditions and the fact that theoretically it involves two crack paths growing in opposite directions starting from the tips of the notches. Furthermore, this will give us comprehension

Property	Notation used	Value
Young Modulus	E	30 GPa
Poisson ratio	ν	0.2
Tensile strength	σ_0	2 MPa
Fracture energy	G	$100\text{J}/m^2$

Table 2.2: Material properties for 4PBT

about the development of these crack paths at the same time and will reproduce a common behavior in the mechanical engineering field.

2.4.2 Meshing

Since the main goal of the strategy is to avoid mesh size dependence, one important step is to create different meshes to work with. Our needs are:

- Good adaptability to the physical response of the material. The mesh has to focus on important parts for the deformation process, therefore a fine mesh will be seek on these regions and coarse mesh may be used in areas where is well known that there are not important effects for the main problem.
- It is important to take under control the average element size where the damage occurs. Different meshes with different element size are created in order to study its effect.

Four different meshes have been created for this goal. Meshes are created by means of the **ez4u** program. The computational domain is discretized with four different unstructured meshes.

The computational domain is covered with a coarse mesh on both sides, where it is known that the deformation occurs in elastic range, and therefore there is not damage inception. The domain is covered by finer meshes in the area where the damage is tried to be captured. From this moment and so on, the meshes are named by its average mesh size in the interesting area to capture the damage. For quadrilateral elements, the mesh average size h is computed as

$$h = \sqrt{A} \tag{2.19}$$

where A is the element area. This expression directly shows the relation between the average area and the average considered size of an element. In figure 2.14 different meshes with their average size are presented.

2.4.3 Material properties

Material properties will be adapted for the resolution of the problem. In order to achieve realistic results and fasten calculations some assumptions are introduced to the material properties. First of all we define a second material, different from the main one described

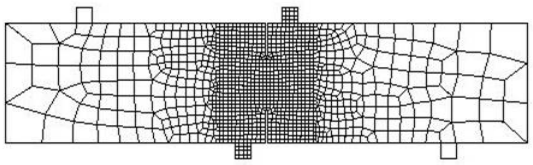

(a) MESH 4: h=10 mm, 1177 elements

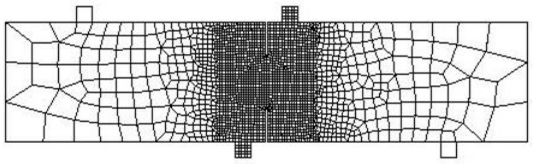

(b) MESH 3: h=7 mm, 2112 elements

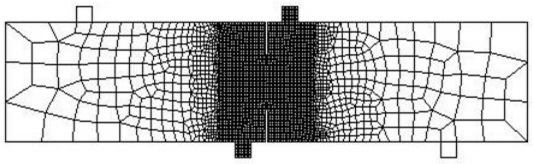

(c) MESH 2: h=5 mm, 3948 elements

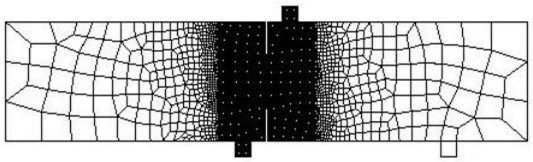

(d) MESH 1: h=3.5 mm, 7377 elements

Figure 2.14: Different meshes used with average mesh sizes in the central part

in table 2.2 and found in the supports where the load is applied. They are supposed to be rigid. We make the assumption that they are made of steel, hence values from table 2.3 are given. As their function is just to transmit loads a high Young modulus value is given to avoid damage in supports. Other properties do not need to be described since deformation for this material occurs in an elastic range.

In order to save computing time another assumption is made. Since the area where the

Property	Notation used	Value
Young Modulus	E	210 GPa
Poisson ratio	ν	0.3

Table 2.3: Material properties for supports in 4PBT

damage is going to take place is known, it is possible to define an elastic material at both sides. All deformation process in the elements located there occurs in elastic range, so the material is considered to be elastic and the elements within this area are not able to be damaged. In figure 2.15 the distribution of the three different materials regarded is depicted to clarify the composition of the whole beam.

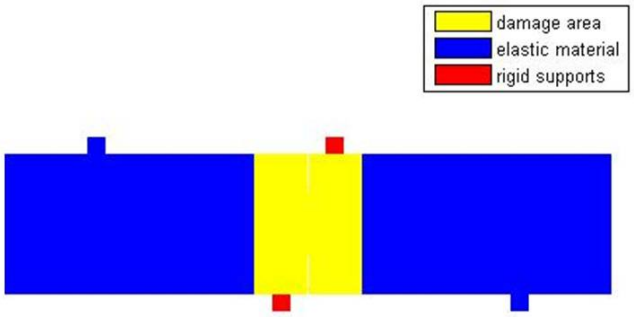

Figure 2.15: Distribution of materials for 4PBT

2.4.4 Boundary conditions

In this section general boundary conditions explained in section 2.2.1 are detailed. Combined boundary conditions for the regularization problem are applied all over the contour of the beam. Mechanical boundary conditions are applied on the domain $\Omega_D = \{\Omega_1 + \Omega_2 + \Omega_3 + \Omega 4\}$ depicted in figure 2.16. Considering the displacement field in the form $\mathbf{u} = (u_x, u_y)$ mechanical boundary conditions are written as

$$\begin{cases} \mathbf{u} = \mathbf{0} & \text{on} \quad \Omega_1 \\ u_y = 0 & \text{on} \quad \Omega_2 \\ u_y = -\delta & \text{on} \quad \Omega_3 \\ u_y = \delta & \text{on} \quad \Omega_4 \end{cases} \tag{2.20}$$

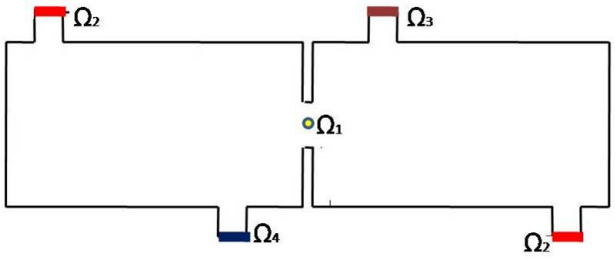

Figure 2.16: Mechanical Boundary Conditions domain for 4PBT

2.4.5 Damage law

Generally described in section 2.2.1, the softening law that affects the softening branch of the problem is mainly controlled by the softening parameter H_S. Band size has a theoretical limit, Eq. (2.15). Evaluating the limit with the material properties from table 2.2,

$$b \leq \mathcal{L} = 2\frac{EG}{{\sigma_0}^2} \quad \Rightarrow \quad b < 150\text{cm} \tag{2.21}$$

The theoretical restriction also includes the nonlocal definition. This is that damage band size must contain at least two damaged elements and therefore the model may be considered nonlocal. From previous definitions, limits involving element size like in Eq. (2.19) and damage law properties, Eq. (2.21)

$$2h \leq b < 150cm \tag{2.22}$$

Actually just the lower limit has to be taken into account since the upper limit is far to be reached. Note that the lower limit depends on the element size and therefore on the mesh.

This thesis deals with the gradient version. Therefore it is focused on the characteristic length study rather than other parameters such as those ones which control the damage law. Thus, an unique damage law is tried to be defined in order to work with all the different meshes. It is not trivial, since meshes show a moderate level of sensitivity to the damage law 2.3.2.

A case of interest comes with damage laws where the band size parameter is selected very small, close to the lower limit. It produces damage on the central point and the deformation process makes it grow at the same time the other damage bands do it. So, with the same mesh and the same characteristic length we may obtain acceptable results depending on this parameter. This effect is more accused by coarse meshes. In 2.17(a) a wrong inception and growth of the damage may be seen. It is provoked by a value that does not fulfill the restrictions. In 2.17(b) the problem comes with a low value and a coarse mesh.

From the experience of the tested values for this parameter it seems that those ones which allow to obtain better realistic results are those ones that are close to the lower re-

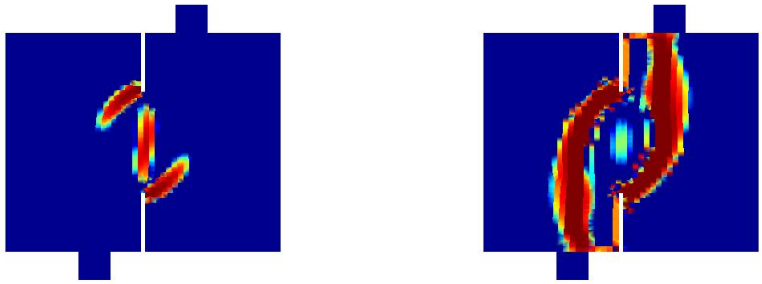

(a) $h = 7$ mm and $b = 13$ mm $b < 2h$ (b) $h = 7$ mm and $b = 15$ mm $b > 2h$

Figure 2.17: Central damage, $l_s = 0.2$

striction, this is $2h \leq b$. The reason is that low values give a softer response in the softening branch and a better approximation to the solution presented in [3], the example that is tried to be reproduced. High values give an excessive straight falling of the softening branch of the damage law, not realistic, and also present problems regarding the convergence. They have to be understood as the complex convergence that occurs using Newton-Raphson methods when a high slope is tried to be captured. Nevertheless, in coarse meshes, if the value is really close to the restriction, damage may appear in the central point.

This damage has to be understood as a loss of symmetry of the problem. The four point bending test presented is a symmetric problem, with a theoretical symmetric field of displacements around the central point. It is reminded that the central node is imposed to be fixed. If the solution of the problem was completely symmetric, the central node would remain exactly at its place and no damage would appear. The mesh is randomly generate and therefore no symmetric distribution of the nodes is expected. In a non symmetric simulation, the central node would be moved if it was under free deformation, but it is imposed to be fixed and then stresses appear and the inception of the damage is found. Once the inception of the damage is produced, since it grows monotonically by its definition, is spread to the elements around. This seems to be the reason why coarse meshes present more sensitivity to this effect. At the end, the effect of a low value for b makes the softening branch be softer and this means a general smoother response to the load and it seems to be related with the appearance of damage in the central point.

2.4.6 l_s as a restrictive variable

The wrong selection for this variable may drive to physically not acceptable results. As seen in section 2.3.2, in the following some not acceptable results obtained are presented in order to show restrictions given by the parameter l_s. The excessive effect of the regularization may provoke the inception of damage in some areas that are supposed to be non damaged, such as the central point and some points along the contour.

First of all, results with null characteristic length are presented. Damage is shown in figure 2.18 and force-deflection plot regarding the three different meshes in figure 2.19.

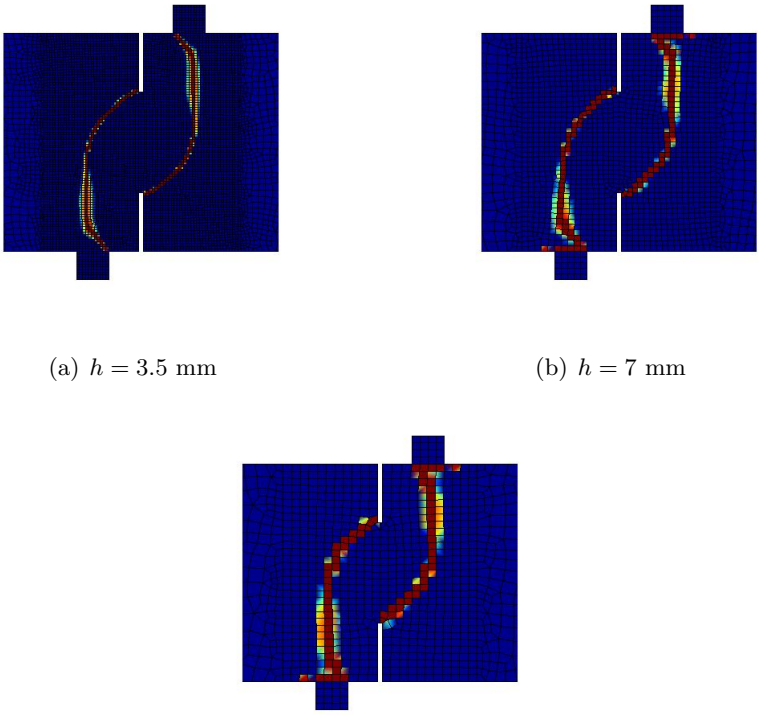

(a) $h = 3.5$ mm

(b) $h = 7$ mm

(c) $h = 10$ mm

Figure 2.18: 4PBT: damage plots with a local model

As seen in damage and force-deflection plots, as the element size becomes smaller the damage takes place in a smaller area. The area under the force-deflection curve is the dissipated energy through the deformation process, and also becomes smaller with an smaller element size. This example clarifies that with no regularization effect the damage takes places in a vanishing volume and therefore fully mesh dependence is observed.

Now the adequate range of values for the characteristic length is discussed. Figure 2.20 shows an excessive or insufficient smoothing effect. For the first case, in figure 2.20(a) damage encounters a high stress area belonging to the tip of the notches and is attracted towards them. Excessive regularization effect makes the damage band grow on that wrong direction and even join the tip of the notch instead of growing vertically. This excessive effect leads to a circular damage band shape and a wrong physical result. On the other hand, figure 2.20(b) shows the opposite effect. An insufficient regularization drives to the depicted damage plot. The width of the damage band contains more than one element but

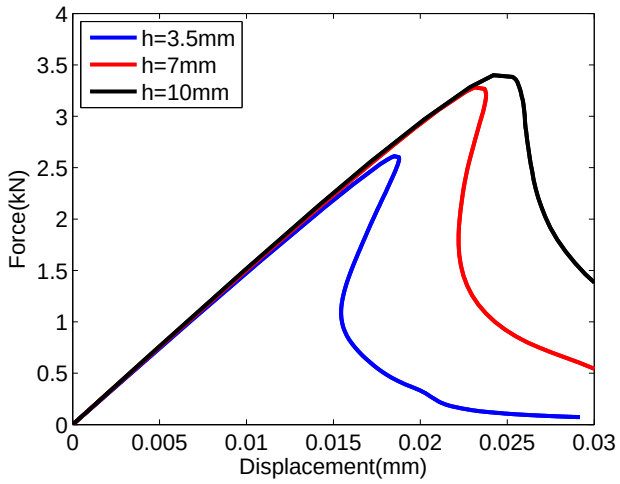

Figure 2.19: Force-deflection in local model for meshes 2, 3 and 4

it is not enough to reproduce a reasonable physical meaning. The value of the characteristic length must be increased. The example shows how with the same simulation in terms of material a different solution is obtained. The role of l_s is to avoid differentiation among different meshes.

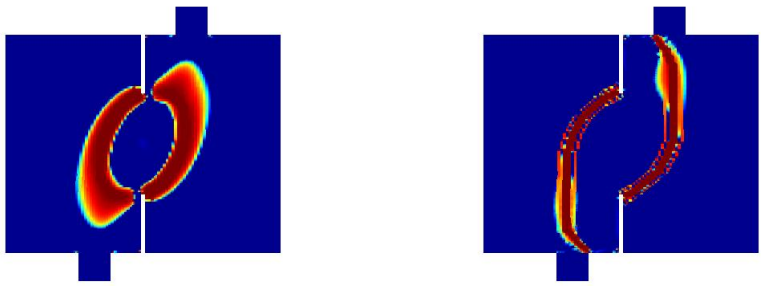

(a) $h = 3.5$ mm, $l_s = 0.3$ (b) $h = 5$ mm, $l_s = 0.05$

Figure 2.20: Excessive and insufficient regularization in 4PBT

To sum up, the characteristic length value has to be determined by an inspection of the obtained results, deciding which one fits the most the physically expected result. Low values close to $l_s = 0$ make the model be not regularised enough, and large values($l_s > 0.2$) provoke an excessive regularization effect. Both situations lead to non physically acceptable results. After many simulations is concluded that, for this problem and for these meshes, characteristic length values from $l_s = 0.13$ to $l_s = 0.18$ lead to more realistic results.

2.4.7 Results

First of all, a detailed solution for a case is presented. The following case of study is developed for a fine mesh in order to present general results and the complete process of deformation. This example is developed with the values of $l_s = 0.15$ and $b = 1$. The mesh has an average size on the central part of $h = 3.5$ mm.

The damage starts on the tip of the notches and grows towards the opposite support. The fact that the notches are placed in the center as an opening of the beam has the clear objective of provoking the damage inception there, as this area becomes highly stressed. As shown, the crack path in the mesh progresses with almost central symmetry with the central point. Note that these two crack paths turn vertically when they reach the action lines of the reactions of the supports where the load is applied.

When the crack paths reach this point, they also show some spreading of damage towards the tip of the notch. This is not a pathological effect of the mesh, since the mesh is built with the same average element size here like along the damage band. Many results show that the effect of the regularization for itself provokes this spreading in highly stressed areas. This effect may be seen in terms of force-deflection curve on the picture 2.23. It is found in deformations between $\delta = 0.035 - 0.045$ mm, where a soft increasing stiffness within a continuous loss of stiffness is observed.

In order to reduce it, a lower value for the characteristic length has to be considered. But it is also true the fact that the lower the characteristic length value is, the lower level of regularization is obtained, and therefore dependence on the mesh may be observed. Therefore in this case a high characteristic length value has been adopted. It is on the threshold of the acceptable results in order to show the potential applicability of this method to this example. Simulation is stopped at the value of $\delta = 0.06$ mm because the deformation process is done and the damage band reaches the opposite side. Further deformations, like in figures 2.24, show an inception of the damage along the free contour, that makes no physical sense, so $\delta = 0.06$ mm is considered to be the final result. Depicted area corresponding to the damage plots presented here is showed in figure 2.21.

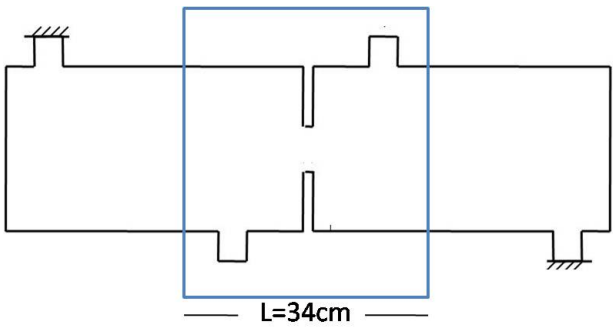

Figure 2.21: Damage plot area for 4PBT

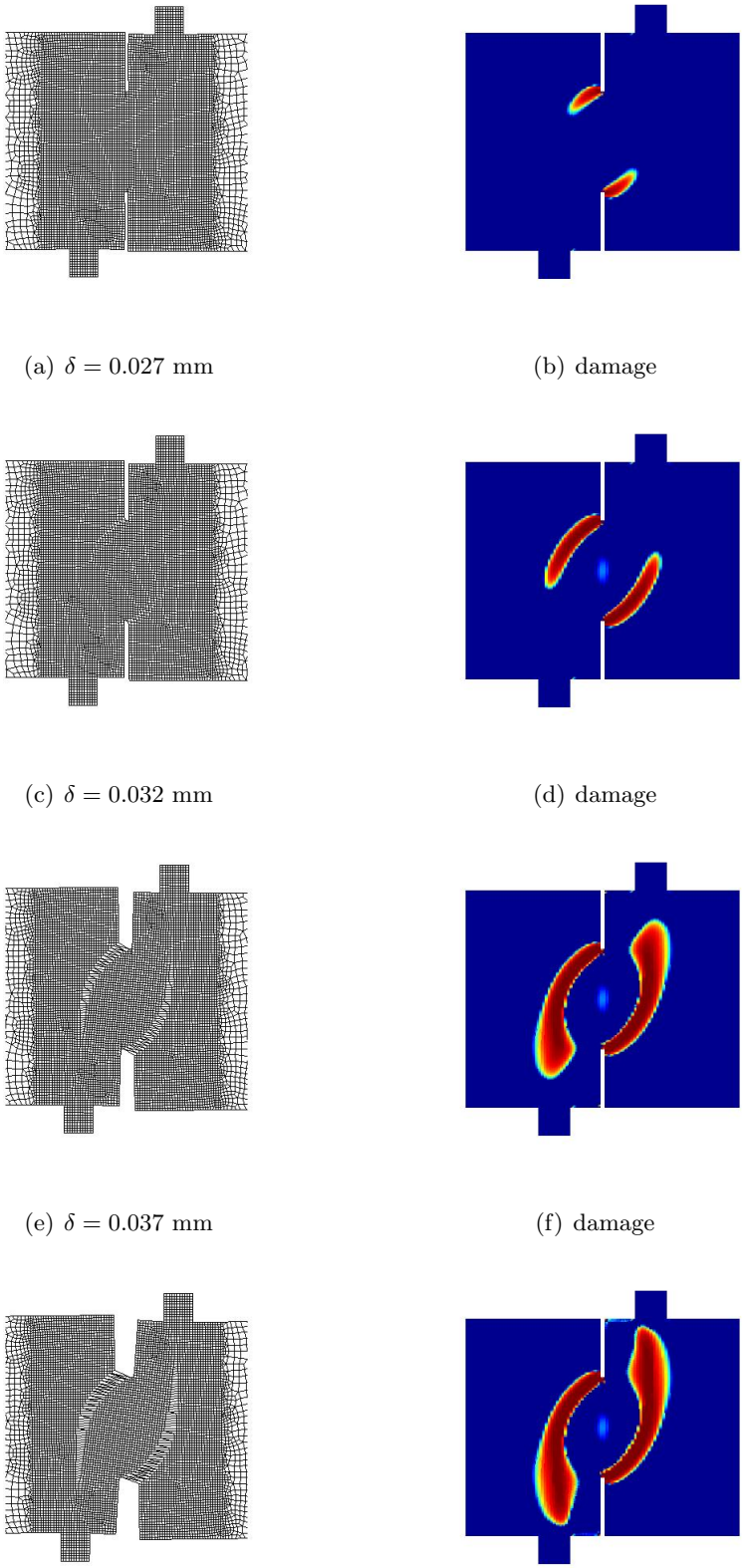

(a) $\delta = 0.027$ mm (b) damage

(c) $\delta = 0.032$ mm (d) damage

(e) $\delta = 0.037$ mm (f) damage

(g) $\delta = 0.045$ mm (h) damage

Figure 2.22: 4PBT: deformation and damage

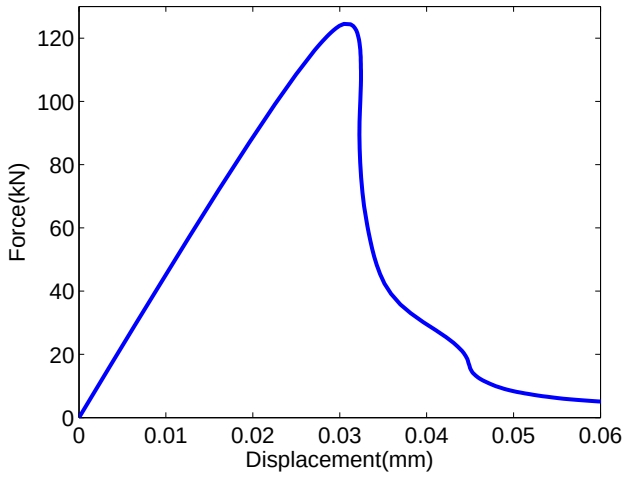

Figure 2.23: Force-deflection for 4PBT

Results from two different meshes are compared in order to see whether the regularization effect achieves the goal or not. The most restrictive parameter to develop this study is b, once l_s range is known. Regarding the lower restriction, Eq. (2.22) and the influence of this parameter, it has to be at least $2 \cdot h_{max}$. In this analysis, meshes 1 and 2 are used, see meshes depicted in figure 2.14. They are chosen because they are the finest ones. The largest element size belongs to mesh 2, and it has an average mesh size of $h = 5$ mm. Therefore the minimum value for b, regarding section 2.4.5 is 10 mm. The characteristic length for these simulations is set to $l_s = 0.15$. The picture 2.24 shows deformation and damage for both meshes at the point that the supports reach a vertical displacement of $\delta = 0.068$ mm, considered to be the final stage of the process.

No mesh dependence on the damage plots is observed in these analysis. Crack paths follow very closely the same path on the two different meshes, and in both cases more than one element is involved. So it is not appreciated any mesh dependence that may take control over the process. Both force-deflection plots are presented in figure 2.25 for the analysis.

The plots show similar curves, presenting the same process, but they are not completely overlayed. The estimated relative error committed, evaluated in the peak force for both curves is

$$\epsilon = \frac{F_{h=5} - F_{h=3.5}}{F_{h=3.5}} = 0.027. \tag{2.23}$$

Therefore an error around 2.7% is committed. The ratio of the average mesh size between the two meshes is 1.42.

From this example is concluded that the gradient version is stable with the right parameters, works well with this problem and gives an acceptable relative error, expected to be decreasing with the mesh size.

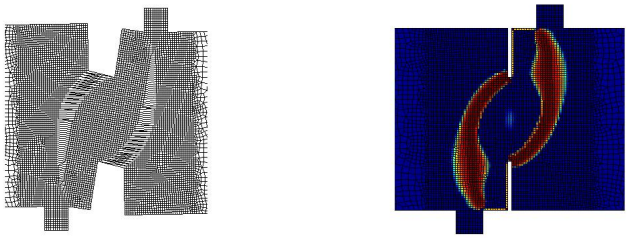

(a) $\delta = 0.068$ mm, mesh 1 (b) damage on mesh1

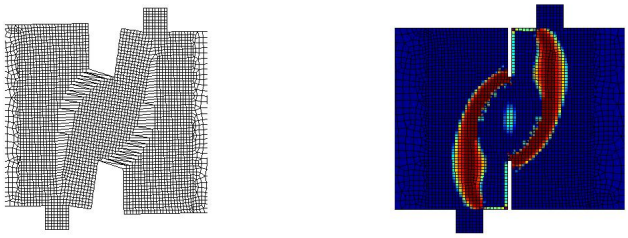

(c) $\delta = 0.068$ mm, mesh 2 (d) damage on mesh2

Figure 2.24: Comparison between mesh1 and mesh2

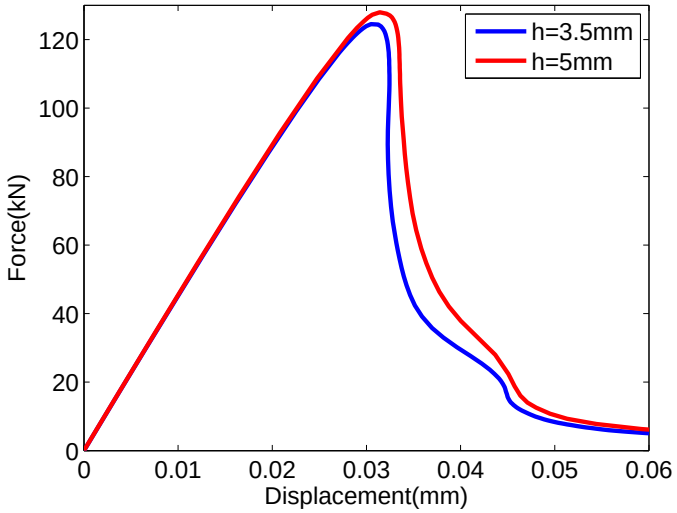

Figure 2.25: Force-deflection comparing mesh1 and mesh2

2.4.8 Other mechanical boundary conditions

A different definition of the boundary conditions gives a complete different result, as the problem becomes a different one. All parameters must be reconsidered for every case. For instance, there is a huge difference between an isostatic and a not isostatic case. Within mechanical boundary conditions, Dirichlet boundary conditions must be described on Ω_D. The domain is detailed in section 2.4.4.

Other mechanical boundary conditions consist of fixed supports, and leaving free the central node. In terms of the Dirichlet domain, then mechanical boundary conditions are written as

$$\begin{cases} \mathbf{u} = \mathbf{0} & \text{on} \quad \Omega_2 \\ u_y = -\delta & \text{on} \quad \Omega_3 \\ u_y = \delta & \text{on} \quad \Omega_4. \end{cases} \tag{2.24}$$

This new formulation for the mechanical boundary conditions leads to a different problem. Once the highest force point in the force-deflection curve is reached, a locking effect starts and keeps the beam gaining deformation, increasing force while the damage is barely increased. This situation gives the right deformation but not the right damage and stress growth. Figure 2.26 regards the maximum damage observed.

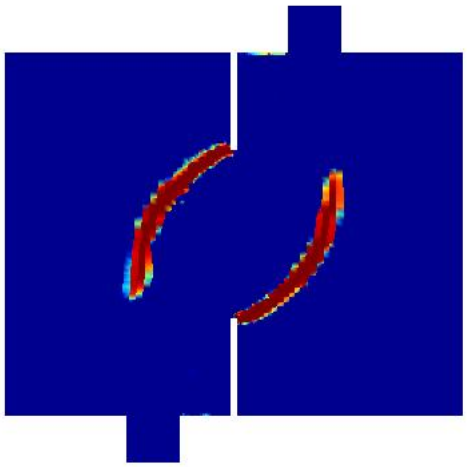

Figure 2.26: Locked damage

The problem of locking acts when some part of the domain carries increasingly more and more load and the general behavior of the beam changes. The damage band grows from the notches towards the opposite support but once reached the depicted point is stopped and it continues carrying load but the damage band is not developed anymore.

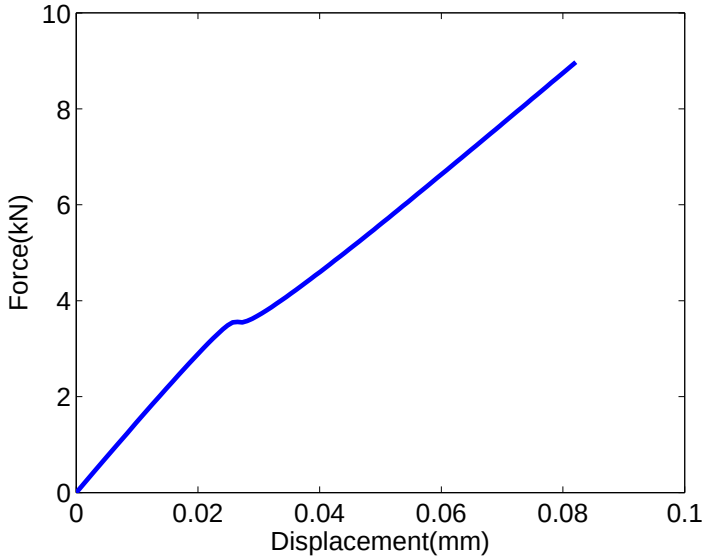

Figure 2.27: Force-deflection observed in the support

The fact of changing boundaries makes the problem be hyperestatic and some tensions appear on the locked boundaries. For itself this is not a problem, since tensions on the boundaries may be computed as well, but in our case this situation gives us a complete different behavior for simulation since convergence problems are found from the beginning of the plastic regime and it is crashed at the depicted point. The force-deflection curve up to this point for the supports is depicted in 2.27. It is clearly observed that the curve does not belong to a softening damage model, and somehow other tensions appeared on the locked boundary have to be taken into account. This problem has tried to be solved considering Von Mises criterion instead of Truncated Rankine and several different types of element mesh with no success.

However, the presented model does not work well with the hyperestatic case here presented.

Chapter 3

Concluding remarks and future work

3.1 Concluding remarks

- In this work a continuous strategy is used to model the process of failure of a material. It regards the first stages of failure, considering damage inception and its propagation.

- With a local continuous technique, the solution of the problem completely depends on the chosen mesh. The damage occurs in a vanishing volume as the element size becomes smaller. In order to avoid mesh dependence a regularization technique is considered. The implicit gradient version of a nonlocal damage model based on non-local displacements is used. The state variable is defined by means of the Truncated Rankine criterion. As shown in this work, the definition of the boundary conditions is not easy for the regularisation problem. Combined conditions are imposed as the solution.

- A three-point bending test analysis is carried out in order to clarify the model and have a good understanding. It is selected due to its simplicity and because it represents a well studied behavior by many authors. For this purpose, a unique mesh is generated and the analysis is done. The difference between a local and a nonlocal model is clearly shown.

- Then a four-point bending test is carried out. It is selected because this problem involves two crack paths at the same time. Both crack paths are captured and the global force-deflection law is successfully obtained. In order to check the avoidance of mesh dependence four different meshes are used and different analysis are carried out. It is achieved with an adequate characteristic length l_s and an adequate damage band size parameter b. Both parameters are deeply studied in this work.

- Behavior for more complex mechanical boundary conditions like locked boundaries that introduce hyperestatic degrees to the problem present important convergence problems. Several damage laws and criterions for the definition of the state variable

such have been tested with no success.

- In conclusion, by this work is concluded that for the four-point bending test, the gradient version based on nonlocal displacements is stable with the right l_s and b parameters, and is able to avoid mesh dependence.

3.2 Future work

Some issues come from the presented work and are interesting to be studied as a next step:

- By now, the nonlocal used technique has been tested for the four-point bending test. Other examples of failure involving multiple cracks could be studied using the same technique.
- So far a first stage of the entire process of failure of the material has been carried out. When the damage is important, real discontinuities appear and the body may be separated in two parts. It is time to change the strategy. Real discontinuities must be incorporated to the model in this second stage. This is, the implementation of a discontinuous technique. The first step is to compute the crack path and introduce it through the structure as a potential opening.
- The presented model deals with two-dimensional applications. Furthermore, three-dimensional applications may be studied.

Bibliography

[1] Lemaitre J and Chaboche J.-L. Mechanics of solid materials. *Cambridge university press*, 1990.

[2] Simone A. Explicit and implicit gradient-enhanced damage models. *Revue Européenee de Génie Civil*, 11:1023–1044, 2007.

[3] Cervera M, Chiumenti M, and Codina R. Mesh objective modeling of cracks using continuous linear strain and displacement interpolations. *International journal for numerical methods in engineering*, 87:962–987, 2011.

[4] Rodríguez-Ferran A, Morata I, and Huerta A. A new damage model based on non-local displacements. *International Journal for Numerical and Analytical Methods in Geomechanics*, 29:473–493, 2005.

[5] Rodríguez-Ferran A, Morata I, and Huerta A. Efficient and reliable nonlocal damage models. *Computer methods in applied mechanics and engineering*, 193:3431–3455, 2004.

[6] de Borst R, Pamin J, Peerlings R.H.J., and Sluys L. On gradient-enhanced damage and plasticity models for failure in quasi-brittle and frictional materials. *Computer mechanics*, 17:130–141, 1995.

[7] Tamayo-Mas E. Continuous-discontinuous models of failure based on non-local displacements. Master's thesis, UPC, 2009.

[8] Möes N, Dolbow J, and T. Belytschko. A finite element method for crack growth without remeshing. *International journal for numerical methods in engineering*, 46:131–150, 1999.

[9] Jirásek M. Damage and fracture in geomaterials. *Revue Européenee de Génie Civil*, 11:977–991, 2007.

[10] Jirásek M and Marfia S. Nonlocal damage models: displacement-based formulations. In *Computational Modelling of Concrete Structures*, 2006.

[11] Geers M.G.D., de Borst R, and Peerlings R.H.J. Damage and crack modeling on single-edge and double-edge notched concrete beams. *Engineering Fracture Mechanics*, 65:247–261, 1999.